SCIENCE CHINA
Information Sciences

• RESEARCH PAPER •

August 2017, Vol. 60 082403:1–082403:9
doi: 10.1007/s11432-016-0645-2

A micro-array bio detection system based on a GMR sensor with 50-ppm sensitivity

Cheng ZHU[1], Lei ZHANG[1]*, Jinwen GENG[1], Xizeng SHI[2] & He QIAN[1]

[1]*Institute of Microelectronics, Tsinghua University, Beijing* 100084*, China;*
[2]*Bosh Biotechnologies, Ltd., Dongguan* 523808*, China*

Received September 29, 2016; accepted November 21, 2016; published online April 24, 2017

Abstract Bio detection is widely utilized in hospitals and laboratories. However, conventional bio detection methods suffer from long detection time, complex operation, and low sensitivity, and these issues prevent their use in point of care testing (POCT) applications. Microelectronic bio detection methods are proposed to overcome these issues. Bio detection based on a micro-electronic technique allows easy integration of a system, leading to a fast detection speed and simple operation. In this work, a fully microelectronic bio detection system including a sensor design, a read-out strategy, and data processing is proposed based on a GMR biosensor. A GMR sensor chip is designed and different passivation layer thicknesses are tested to improve sensitivity. A 40 nm thickness passivation is realized to produce the largest response without oxidization and breakdown. In order to integrate the read-out circuit and simplify operations, a 4-channel read-out biochip is designed and fabricated, and this exhibits a super-low output noise corresponding to −116.84 dBm/Hz at the operation frequency. This means that the noise only approximately corresponds to the signal level of five magnetic nanoparticles with a diameter of 200 nm. A reference sensor is also utilized to cancel the unwanted signal and reduce common-mode noise and error to improve sensitivity. Measurements indicate that 90% suppression is achieved. The measurements also reveal that a sensitivity of 50 ppm is achieved with the proposed GMR bio detection system.

Keywords giant magnetoresistance (GMR), biosensor, magnetic nanoparticle (MNP), small signal extraction, sensitivity

Citation Zhu C, Zhang L, Geng J W, et al. A micro-array bio detection system based on a GMR sensor with 50-ppm sensitivity. Sci China Inf Sci, 2017, 60(8): 082403, doi: 10.1007/s11432-016-0645-2

1 Introduction

Point of care testing (POCT) is an extremely issue in recent years. It requires fast detection speed, easy operation, and high sensitivity. Conventional bio detection methods, such as enzyme-linked immunosorbent assay (ELISA) [1, 2] and fluorescent method [3], suffer from low sensitivity, severe body fluid interference, and complex front-end biochemical operations prior to detection. This in turn leads to a long pretreatment time and complex operations and prevents their usage in POCT applications.

Novel bio detection methods based on microarray techniques are widely researched for POCT applications [4, 5]. Novel bio-microarray detection techniques use electronic circuits to read-out a bio signal, and thus they are fast, multi-target oriented, cheap, and user-friendly.

* Corresponding author (email: zhang.lei@tsinghua.edu.cn)

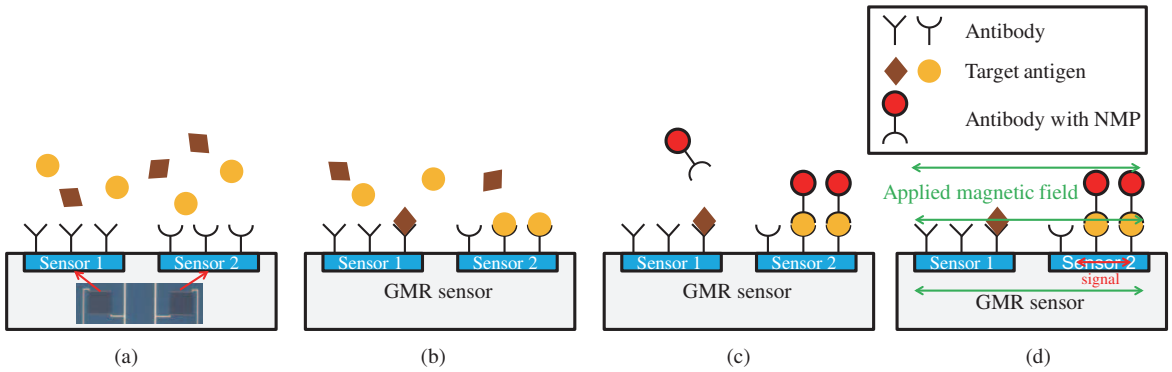

Figure 1 (Color online) Steps in GMR biosensor detection. MNPs are utilized to tag analytes and change the resistance of the sensor in an applied magnetic field.

Novel bio-microarray techniques can be divided into two categories, namely labeled and label-free categories. Labeled techniques feature a higher sensitivity with a wider application when compared with label-free techniques [6–8]. Novel labeled bio-microarray technologies utilize magnetic nanoparticles (MNPs) to translate a bio signal into an electronic signal. Magnetic tags feature lower body fluid interference when compared with other tags utilized in conventional detection techniques such as fluorescence tags. This is because there are less magnetic interferents in human body fluid, and this implies simple front-end biochemical operations and high sensitivity.

Existing bio-microarray detection techniques, such as hall and inductor methods, suffer from various limitations. A hall micro-array technique needs an array of hall sensors to detect a single target [9, 10], which means that a trade-off between sensor chip size and dynamic range is necessary. Additionally, a high the sensor array size is required to detect a single target, and thus it is expensive to achieve multiple target applications in hall sensor micro-array bio detection. An inductor micro-array technique detects a resonant frequency change. The magnetic field of an inductor can be changed by MNPs on the surface of the sensor, and this leads to a resonant frequency change. However, the reported sensitivity of an inductor bio-microarray is not sufficiently high for bio detection applications [11]. When compared with hall and inductor solutions, a bio-microarray based on a GMR sensor involves both high sensitivity and a large dynamic range. Thus, it has gained immense popularity in recent years and was explored by several extant studies [12, 13]. A study by de Boer [14] utilized a 1 MHz current to read a 50 kHz GMR signal and retain flicker noise. However, this implies that a demodulation system is necessary. This complicates the system, and it is hard to realize a high 50 kHz magnetic field. A study by Hall [15] used a digital-to-analog converter (DAC) to produce a center tone cancellation signal. However, using a DAC to produce a center tone cancellation signal indicates that it is not possible to cancel an unwanted signal on the side tone in order to reduce the signal noise ratio.

It is not possible for a GMR sensor to directly detect a biological signal. Thus, it is necessary to translate a biological signal into an electrical signal. Figure 1 shows the detection steps. The surface of a sensor and MNPs are first modified with a specific antibody. A target antigen and the modified antibody combine by antigen-antibody reaction when target antigens are introduced. Thus, MNPs are fixed on the top of a sensor. The application of an AC magnetic field to the sensor leads to the production of a small magnetic field in the same direction by the MNPs. The resistance of the GMR sensor changes with the magnetic field, and the resistance change is read-out to calculate the number of MNPs on the top of the sensor. The specificity of the antigen-antibody reaction ensures that only the target antigen leads to antigen-antibody reaction and fixes the MNPs on the top of the sensor. A MNP on the top of the sensor corresponds to a target antigen on the top of the sensor. The number of MNPs are read-out to calculate the number of target antigens.

In this work, a complete biodetection system and scheme is proposed and includes fabrication of the sensor, small signal extraction strategy, and data processing. A passivation layer with different thicknesses is tested to achieve a maximal response. The results indicate that a 40 nm thick passivation layer can achieve a maximal response without oxidation and breakout. A 4-channel readout biochip is designed

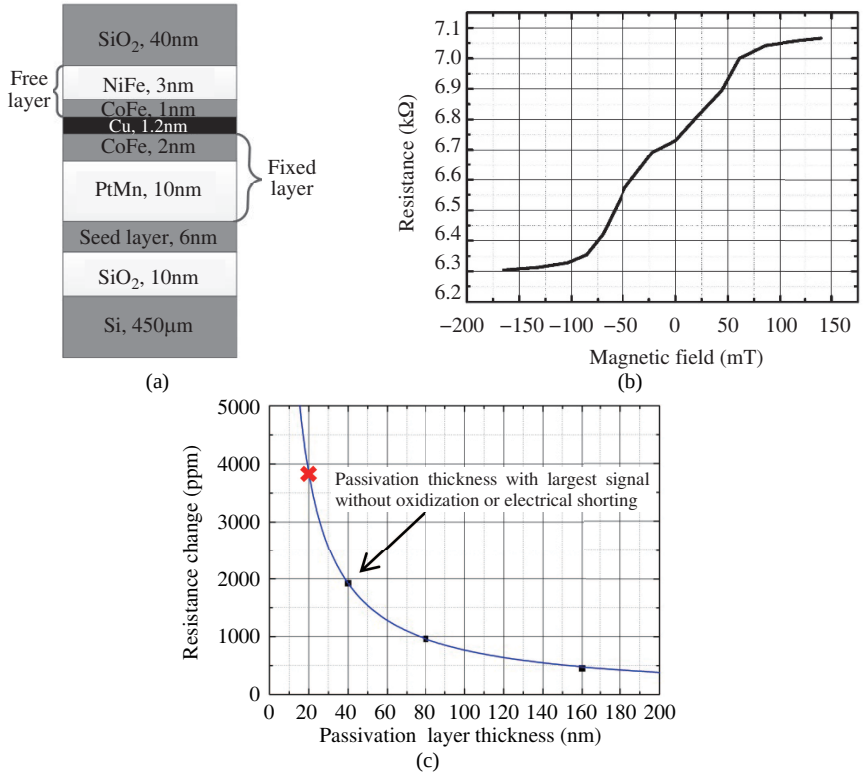

Figure 2 (Color online) (a) Multilayer structure of the proposed GMR sensor; (b) GMR sensor resistance relative to the applied magnetic field; (c) signal versus passivation layer thickness.

for further miniaturization of the system. The biochip exhibits a significant well noise performance that only corresponds to −116.84 dBm/Hz at the operating frequency, which implies that the noise is only at approximately a signal level corresponding to that of five magnetic nanoparticles with a diameter of 200 nm. A reference sensor is used for cancellation to reduce common-mode noise and drifting and especially temperature drifting and time drifting. With the reference sensor cancellation scheme, a 90% suppression of the common-mode noise and error is achieved by measurement. Based on the proposed system, a sensitivity of approximately 50 ppm is achieved, and this implies a sensitivity that approximately corresponds to that of 600 MNPs with a diameter of 200 nm for a 120 μm×120 μm sensor.

2 Fabrication

The proposed GMR biosensor is a NiFe/CoFe/Cu/CoFe/PtMn multilayer structure fabricated on the seed layer as shown in Figure 2(a). The resistance of GMR sensor is changed by a magnetic field through the sensor. The curve of GMR sensor resistance relative to the applied magnetic field is shown in Figure 2(b). The maximum magneto-resistance ratio of the GMR sensor is approximately 10%. Both the applied magnetic field and the magnetic field produced by MNPs lead to a resistance change. In the proposed system, the applied magnetic field and magnetic field produced by MNPs are in the same direction and at the same frequency. The MNP signal is added to the signal of the applied magnetic field.

On the surface of the sensor, a 40 nm thick SiO_2 layer is fabricated to prevent oxidization and electrical shorting. The relationship between passivation layer thickness and the signal is shown in Figure 2(c). The thickness of the passivation layer considers the requirement of sensor protection and sensor sensitivity. A thinner passivation layer can achieve a closer proximity between the MNP and the sensor leading to higher sensitivity but resulting in easier electrical breakdown and sensor oxidation. As shown in the figure, the MNP signal almost exhibits a reciprocal relationship with the sensor passivation layer thickness. A 20 nm thick passivation sensor depicted in the left side of Figure 2(c) is unusable because of the oxidization of the GMR sensor. Additionally, a 40 nm thick passivation layer is sufficiently thin since the utilized MNP

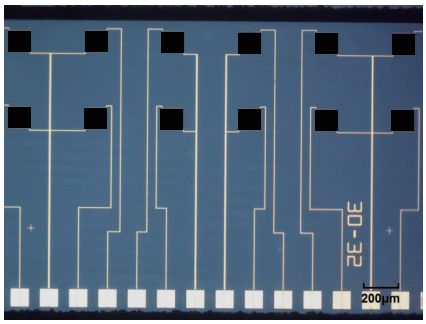

Figure 3 (Color online) The GMR biosensor chip consists of 12 independent sensors.

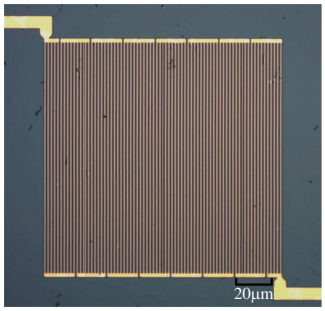

Figure 4 (Color online) The GMR biosensor is fabricated in parallel.

diameter corresponds to 200 nm. This implies that the distance from the center of MNPs to the sensor is mainly determined by the MNP diameter. In the proposed structure, the sensor is free from breakdown under a 10 Vpp alternating current (AC) stress while ensuring the wetness of the sensor surface due to a phosphate buffer saline (PBS).

In order to support multiple target applications, 12 separate GMR sensors are fabricated in a biosensor chip as shown in Figure 3. The physical size of each sensor corresponds to 120μm×120μm considering the trade-off between the statistical fluctuation of MNP distributions and an uneven magnetic field effect during detection. A further increase in the area of the GMR sensor induces an uneven magnetic field effect over the entire detection zone, which means that MNPs located in different places in the sensor produce different signals. Furthermore, a further decrease in the area results in severe statistical fluctuations in the distributed MNPs, and therefore degrades the sensitivity. Moreover, 12 separate GMR sensors imply that 12 different antigens are simultaneously detected. The sensor size and distance between difference sensors (which is subject to spotting restrictions) are fixed, and thus the chip size is mainly determined by the number of sensors. Additionally, 12 separate GMR sensors can fit most applications and the chip size is moderate, thereby ensuring that the cost does not increase.

Twelve sensors are divided into three groups each with a common port. Specifically, the middle four sensors are divided into two groups, each with a common port to satisfy the requirement for interfacing with later-stage readout circuits. The distance between each sensor is 300 μm due to the biomodification requirement for multiple target detection application. The distance between a sensor and pad considers the biochemical operation. In order to overcome the interference of the pad during solution flow through the chip, an 870 μm space is used between the sensor and pad. With respect to the above design restraints, the total size of the sensor corresponds to 2500 μm × 1541.1 μm.

The structure of a single sensor is shown in Figure 4. It contains 75 GMR lines and each set of 5 lines is connected in parallel to reduce the resistance to approximately 7 kΩ. The GMR sensor is laid out from two opposite angles. The structure considers the size of the sensor and the resistance of the sensor wherein it is necessary to keep the size of the sensor while reducing the resistance of the sensor because higher resistance implies higher thermal noise, which in turn reduces the sensitivity.

3 Principle

Figure 5 shows the read-out strategy of a GMR biosensor. An AC voltage is applied to the GMR sensor to read out the resistance change of the GMR sensor. The resistance of GMR sensor changes with the applied magnetic field, and thus the current flowing through the sensor is calculated by using the following expression:

$$\begin{aligned} I_{\mathrm{GMR}}(t) &= \frac{V\cos(2\pi f_c t)}{R_0 + \Delta R_0 \cos(2\pi f_s t)} \approx \frac{V}{R_0}\cos(2\pi f_c t) - \frac{V\Delta R_0}{R_0^2}\cos(2\pi f_c t)\cos(2\pi f_s t) \\ &\approx \frac{V}{R_0}\cos(2\pi f_c t) - \frac{V\Delta R_0}{2R_0^2}(\cos(2\pi(f_c + f_s)t) + \cos(2\pi(f_c - f_s)t)). \end{aligned} \tag{1}$$

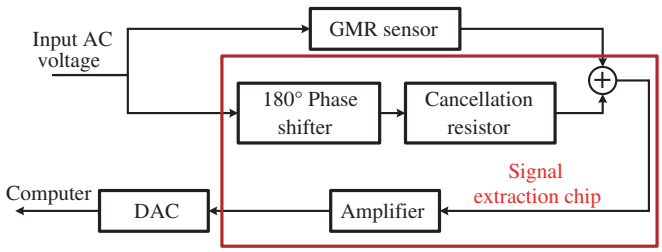

Figure 5 (Color online) Read-out strategy of the GMR biosensor.

In the expression, $I_{\mathrm{GMR}}(t)$ denotes the current flowing through the sensor, f_c denotes frequency of the applied AC voltage, f_s denotes frequency of the applied AC magnetic field, and V denotes amplitude of the AC voltage. Additionally, R_0 denotes initial resistance of the GMR sensor, and ΔR_0 denotes resistance change of the GMR sensor produced by the applied magnetic field and MNPs.

The above expression is simplified to determine a three-peak signal. Frequencies of the peaks correspond to f_c, $f_c + f_s$, and $f_c - f_s$. The peaks are described as a center tone and two side tones. The center tone has the same frequency as the applied AC voltage, and the frequencies of the side tones are f_s away from it. In the system, the GMR sensor acts as a mixer and mixes the magnetic signal with the applied AC voltage frequency to filter high flicker noise at a low frequency.

An AC voltage corresponding to a frequency of 50 kHz is selected to prevent a flicker noise corner, and an AC magnetic field with a frequency of 210 Hz is selected to avoid 50 Hz interferences in the AC electric supply.

The simplified expression indicates that ΔR_0 is only on the side tone, which implies that it is sufficient to extract the side tones and that the center tone is unnecessary. Furthermore, the resistance change in the GMR sensor ΔR_0 is significantly less than the initial resistance R_0, which indicates that the center tone is significantly higher than the side tones. This leads to a high unwanted signal and a prohibitive dynamic range requirement with respect to the following ADC.

A center tone cancellation circuit is designed to fix the issue. The phase of input AC voltage is shifted by 180°, and a cancellation resistor with a resistance close to that of the GMR sensor is used to produce a 180° phase shift center tone current. Subsequently, the cancellation current is added to the current flowing through the GMR sensor. Therefore, the center tone is cancelled by the cancellation signal while the side tones are intact. A 10% mismatch between the resistance of GMR sensor and cancellation resistor is considered. The center tone can be cancelled by a minimum signal of 20 dB.

An amplifier is used to amplify the signal since the signal produced by MNPs is extremely small. For example, a 200 nm diameter MNP only produces a signal that is less than 0.01% of the side tone.

Following these steps, a voltage signal with the required signal on the side tone after center tone cancellation is sent to the ADC for follow-up data processing.

A 4-channel biochip is designed and fabricated with the fore-mentioned read-out strategy as shown in Figure 6. A low-dropout regulator (LDO) and an input amplifier are designed to satisfy the application. The LDO is designed to reduce the supply interference of the control system. The input amplifier is used to amplify the input signal that enhances the signal and suppresses the noise of the following system. A resistor ladder or a reference sensor is utilized in the cancellation circuit. The resistor ladder is designed on a chip with 128 steps. A switch is introduced to control as to whether the resistor ladder or the reference sensor is used for cancellation.

4 Data processing

The ADC samples the output signal from the circuit with a 500 kHz sampling frequency and 1 s sampling time. In order to process the data, FFT is performed with respect to the post-windowed signal, and a

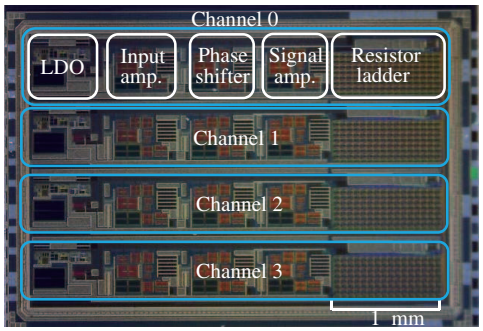

Figure 6 (Color online) 4-channel signal extraction biochip.

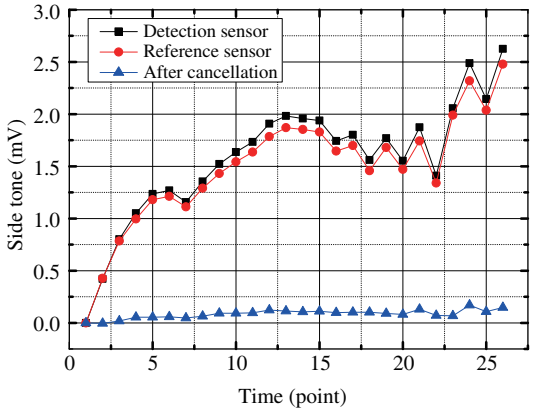

Figure 7 (Color online) Side tone of the detection sensor and reference sensor.

Hanning window is used. The following expression is used to calculate MR and signal levels in ppm [16]:

$$\mathrm{MR} = \frac{4\mathrm{ST}}{\mathrm{CT} - 2\mathrm{ST}}, \tag{2}$$

$$\mathrm{Signal} = \frac{\mathrm{MR}(t) - \mathrm{MR}(0)}{\mathrm{MR}_{\max}}, \tag{3}$$

where CT and ST denote the amplitudes of the center tone and side tones, respectively. There are two side tones, and ST refers to the average of two side tones. In order to recover the center tone, the following expressions are used:

$$\mathrm{CT}_{\mathrm{cancellation}} = \frac{\mathrm{VR}_s}{R_c}, \tag{4}$$

$$\mathrm{CT}_{\mathrm{before\text{-}cancellation}} = \mathrm{CT}_{\mathrm{cancellation}} \pm \mathrm{CT}_{\mathrm{after\text{-}cancellation}}, \tag{5}$$

where R_s denotes amplification resistor in the amplifier, R_c denotes cancelling resistance, and $\mathrm{CT}_{\mathrm{cancellation}}$ denotes cancellation voltage range produced by the cancellation circuit. In the second expression, $\mathrm{CT}_{\mathrm{cancellation}}$ is used to recover the center tone. A negative value is selected if the resistance of GMR sensor exceeds that of the cancellation resistor, and a positive value is selected otherwise. The resistances of the GMR sensor and cancellation resistor are easily detected prior to the test.

Calibrations are performed prior to obtaining the result. The most important calibrations correspond to the source and temperature calibrations. The applied AC voltage is unstable, and thus it must be calibrated. In order to reduce the influence of the source drift, the center tone and side tone are divided by the source rate that is defined as per the following expression:

$$\mathrm{SR}_t = \frac{V_{\mathrm{source}}(t)}{V_{\mathrm{source}}(0)}. \tag{6}$$

A reference sensor is utilized for calibration. A sensor is covered with room temperature vulcanization (RTV) silicone to keep it separate from the MNPs, and it is used as a reference sensor. In the most recent biochip, a sensor with a 2μm-thick passivation layer is used as a reference sensor. The reference sensor receives the same common-mode noise and error as those of the detection sensor including the temperature drift, time drift of the front-end system, and source noise. Figure 7 shows calibration with the reference sensor. The three lines in the figure denote the side tone amplitude of the detection sensor, the side tone amplitude of the reference sensor, and the side tone after calibration, respectively. All three lines are normalized with respect to the starting time. The findings reveal that common-mode noise and error can be suppressed by 90% with the reference sensor. Additionally, the reference sensor simultaneously cancels the side tone produced by the applied magnetic field. This implies that the unwanted signal is reduced and a higher input AC voltage can be applied. A larger input AC voltage increases the signal and suppresses the noise.

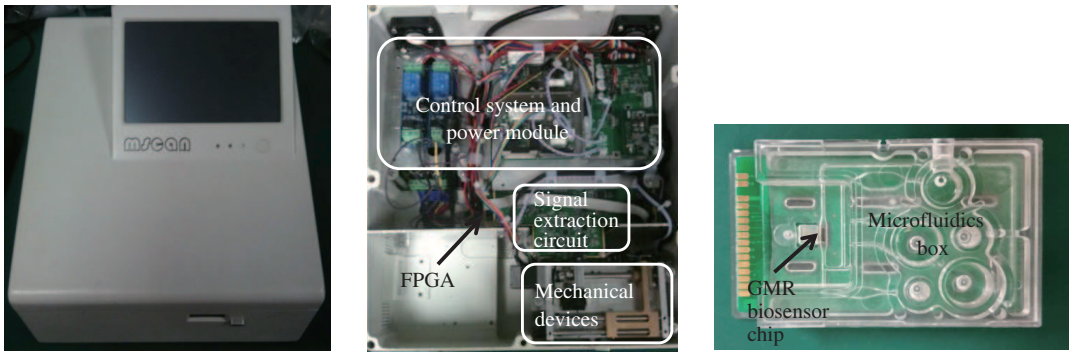

(a) (b) (c)

Figure 8 (Color online) (a) α prototype detector utilizing discrete circuit; (b) the structure of the α prototype detector; (c) the detecting card of the α prototype detector.

5 Results

Figure 8 shows the α prototype detector based on the system and includes the mechanical structure, signal extraction circuit, FPGA, control system, and power module. The signal extraction can be replaced by the 4-channel signal extraction biochip. In detection, the testing card as shown in Figure 8(c) is used for detection. The testing card consists of the GMR biosensor chip, a printed circuit board (PCB), and a microfluidics box. In the biochemical reaction phase, the mechanical devices enable a biochemical reaction on the top of the sensor in the testing card and bind MNPs to the top of the sensor. The MNPs produce a small magnetic field that is superimposed on the applied magnetic field and changes the resistance of the GMR sensor. The resistance change in the sensor is detected by the read-out circuit and sent to the CPU in the prototype detector. Finally, the result is directly shown on the screen.

Figure 9 shows the output noise result of the read-out biochip shown in Figure 6. A resistance is used for testing to prevent the interference of the GMR sensor. The noise power spectral density (PSD) corresponds to -116.84 dBm/Hz at 49.79 kHz. The output noise produces a signal that corresponds to that of approximately five MNPs with a diameter of 200 nm.

It is easier for larger MNPs to sit on the surface of GMR biosensor. Thus, it is hard for the MNPs to wash away, and this causes nonspecific binding and produces an error signal. Smaller MNPs are used to reduce nonspecific binding, and thus MNPs with a diameter of 200 nm are used in the detection. This is the result of a trade-off between single MNP signal and specific binding. A discontinuity exists with respect to the top passivation layer. Therefore, when the GMR sensor is wet, the liquid on the surface leads to a current leakage that can produce a signal as high as several hundred PPM even if distilled water is present on the top of the sensor. Therefore, in the experiment, the top surface of the GMR sensor is kept dry initially, and it is necessary to collect the data after the biochemical reaction following the drying of the surface of the GMR to remove the influence of the solvent. The data curve is shown in Figure 10. The short dash line indicates the surface reaction phase. The surface of the sensor is wet at this time, and thus it is not possible to use the signal for detection purposes. The top of the sensor is kept dry at the beginning and end of the detection, and thus the difference between those in Figure 10 corresponds to the signal produced by MNPs on top of the sensor.

A scanning electron microscope (SEM) is used to observe the number of MNPs on the top of the sensor. Figure 11 shows the MNPs on the top of the GMR biosensor. In the SEM picture, it is estimated that approximately 600 MNPs exist on the top of the sensor.

The relationship between the magnetic signal and number of MNPs with a diameter of 200 nm is shown in Figure 12. A sensitivity of approximately 50 ppm is achieved, and this indicates that approximately 600 MNPs with a diameter of 200 nm exist on the 120 μm $\times$ 120 μm GMR biosensor. Each 200 nm-diameter MNP produces a signal of approximately 0.09 ppm.

Table 1 shows comparisons of the GMR biosensor proposed in this work with other GMR micro-array biosensors. The results indicated that the proposed sensor exhibited a very competitive performance

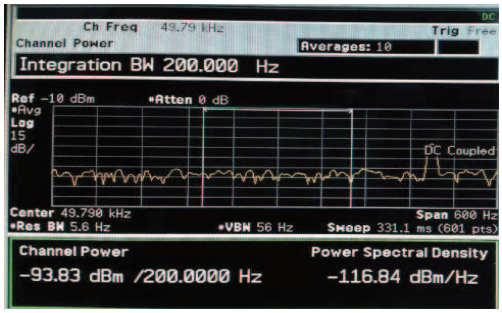

Figure 9 (Color online) Output noise spectrum of the read-out biochip.

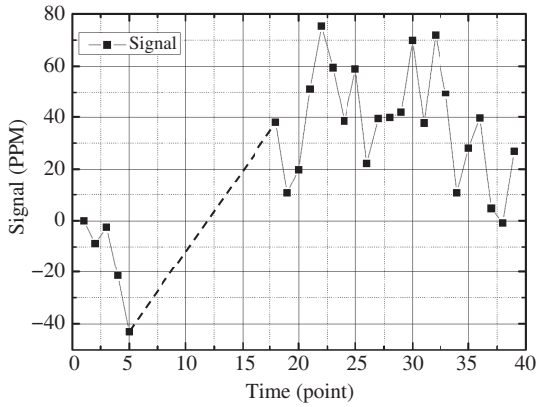

Figure 10 Magnetic signal of the GMR biosensor. The short dash line indicates the surface reaction.

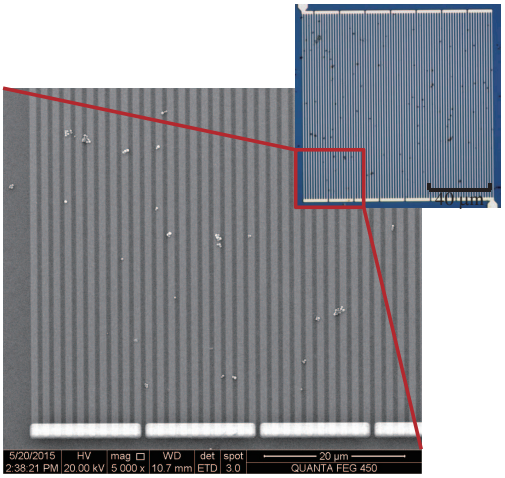

Figure 11 (Color online) The picture on the top right is obtained by an optical microscope. The bottom left picture shows the partial enlarged view of the part in the red circle and is obtained by SEM.

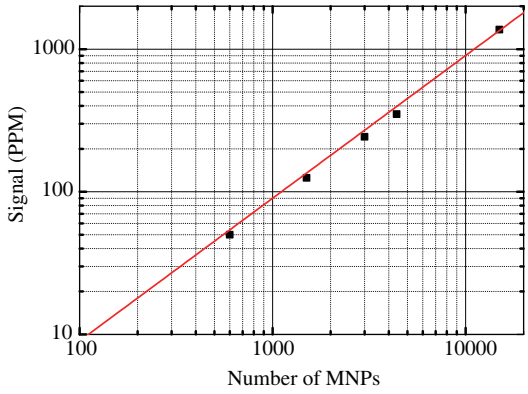

Figure 12 (Color online) Magnetic signal relative to the number of MNPs, each MNP with a diameter of 200 nm produces a signal that approximately corresponds to 0.09 ppm.

Table 1 Comparison with state-of-the-art

Ref.	Sensor type	Sensor size (μm^2)	Target number	MNP diameter (nm)	Min. MNP detectable number N	N Per 10000 μm^2	Dynamic range (dB)
This Work	GMR	120 × 120	12	200	600	416.7	64
[17]	GMR	100 × 100	256	50	2000	2000	70
[18]	GMR	31400	64	2800	10	3.18	42
[19]	LC	120 × 120	8	1000	1	0.69	52.2
[20]	Hall	3 × 4 (30 k sensors)	N/A	4500	13	0.36	53

relative to sensors developed in prior studies.

6 Conclusion

In this work, a complete biodetection system is proposed based on a GMR biosensor and includes sensor design, a readout strategy, and data processing. In the sensor design, a 40 nm-thick passivation layer is fabricated on the surface of the sensor after testing different thicknesses of the passivation layer to achieve the highest signal without oxidation or electrical shorting. A 4-channel biochip is designed based on the readout strategy for miniaturization the system. It can simultaneously readout 4 sensors with a

super low output noise PSD of −116.84 dBm/Hz at 49.79 kHz, which is only approximately equal to the signal of five MNPs with a diameter of 200 nm. A reference sensor is used for calibration to suppress the noise and error during the detection. With respect to the reference sensor, a 90% suppression in the noise and error is achieved as indicated by measurements. The bio detection system is realized by performing an experiment and a sensitivity of 50 ppm is achieved, which translates to approximately 600 magnetic particles with a diameter of 200 nm on a 120 μm × 120 μm GMR biosensor. This result is very competitive relative to the best results achieved by extant studies.

Acknowledgements This work was supported by National Natural Science Foundation of China (Grant Nos. 61204026, 61101001, 61674087), Guangdong's High-Tech Project (Grant No. 2015B020233001), Dongguan's High-Tech Project (Grant No. 2014215102), and Tsinghua University Initiative Scientific Research Program.

Conflict of interest The authors declare that they have no conflict of interest.

References

1 Lequin R M. Enzyme immunoassay (EIA)/enzyme-linked immunosorbent assay (ELISA). Clin Chem, 2005, 51: 2415–2418
2 Leng S X, McElhaney J E, Walston J D, et al. ELISA and multiplex technologies for cytokine measurement in inflammation and aging research. J Gerontol Ser A-Biol Sci Med Sci, 2008, 63: 879–884
3 Weiss S. Fluorescence spectroscopy of single biomolecules. Science, 1999, 283: 1676–1683
4 Yazawa Y, Oonishi T, Watanabe K, et al. A wireless biosensing chip for DNA detection. In: Digest of Technical Papers of IEEE International Solid-State Circuits Conference (ISSCC), 2005. 562–617
5 Garner D M, Bai H, Georgiou P, et al. A multichannel DNA SoC for rapid point-of-care gene detection. In: Digest of Technical Papers of IEEE International Solid-State Circuits Conference (ISSCC), 2010. 492–493
6 Wang Z, Miao J, Xu T, et al. Biosensors based on flexural mode piezo-diaphragm. In: Proceedings of the 3rd IEEE International Conference on Nano/Micro Engineered and Molecular Systems (NEMS), Sanya, 2008. 374–378
7 Zhang L, He X Q, Wang Y, et al. A fully integrated CMOS nanoscale biosensor microarray. In: Proceedings of IEEE Custom Integrated Circuits Conference (CICC), San Jose, 2011. 1–4
8 Manickam A, Chevalier A, McDermott M, et al. A CMOS electrochemical impedance spectroscopy (EIS) biosensor array. IEEE Trans Biomed Circuits Syst, 2010, 4: 379–390
9 Skucha K, Liu P, Megens M, et al. A compact hall-effect sensor array for the detection and imaging of single magnetic bead in biomedical assay. In: Proceedings of the 16th International Solid-State Sensors, Actuators and Microsystems Conference, Beijing, 2011. 1833–1836
10 Besse P, Boero G, Demierre M, et al. Detection of a single magnetic microbead using a miniaturized silicon Hall sensor. Appl Phys Lett, 2002, 80: 4199–4201
11 Wang H, Chen Y, Hassibi A, et al. A frequency-shift CMOS magnetic biosensor array with signle-bead sensitibity and no external magnet. In: Digest of Technical Papers of IEEE International Solid-State Circuits Conference (ISSCC), 2009. 438–439
12 Koets M, van der Wijk T, van Eemerena J T W M, et al. Rapid DNA multi-analyte immunoassay on a magneto-resistance biosensor. Biosens Bioelectron, 2009, 24: 1893–1898
13 Han S J, Xu L, Yu H, et al. CMOS integrated DNA microarray based on GMR sensor. In: Proceedings of International Electron Devices Meeting (IEDM'06), San Francisco, 2006. 11–13
14 de Boer B M, Kahlman J A H M, Jansen T P G H, et al. An integrated and sensitive detection platform for magneto-resistive biosensors. Biosens Bioelectron, 2007, 22: 2366–2370
15 Hall D A, Gaster R S, Osterfeld S J, et al. A 256 channel magnetoresistive biosensor microarray for quantitative proteomics. In: Proceedings of 2011 Symposium on VLSI Circuits (VLSIC), Honolulu, 2011. 174–175
16 Hall D A, Gaster R S, Osterfeld S J, et al. GMR biosensor arrays: correction techniques for reproducibility and enhanced sensitivity. Biosens Bioelectron, 2010, 25: 2177–2181
17 Hall D A, Gaster R S, Makinwa K A A, et al. A 256 Pixel Magnetoresistive Biosensor Microarray in 0.18μm CMOS. IEEE J Solid-State Circ, 2013, 48: 1290–1301
18 Rife J C, Miller M M, Sheehan P E, et al. Design and performance of GMR sensor for the detection of magnetic microbeads in biosensors. Sensor Actuator A-Phys, 2003, 107: 209–218
19 Wang H. Magnetic sensors for diagnostic medicine: CMOS-based magnetic particle detectors for medical diagnosis applications. Microw Mag, 2013, 14: 110–130
20 Skucha K, Gambini S, Liu P, et al. Design considerations for CMOS-integrated Hall-effect magnetic bead detectors for biosensor applications. J Microelectromech Syst, 2013, 22: 1327–1338